R-03-16

Potential impact of colloids on plutonium migration at the Äspö site

Vladimir Cvetkovic, Royal Institute of Technology (KTH)

February 2003

Svensk Kärnbränslehantering AB
Swedish Nuclear Fuel
and Waste Management Co
Box 5864
SE-102 40 Stockholm Sweden
Tel 08-459 84 00
+46 8 459 84 00
Fax 08-661 57 19
+46 8 661 57 19

SKB

ISSN 1402-3091
SKB Rapport R-03-16

Potential impact of colloids on plutonium migration at the Äspö site

Vladimir Cvetkovic, Royal Institute of Technology (KTH)

February 2003

Keywords: Plutonium transport, crystalline rock, Äspö, colloid-facilitated transport, retention, discrete fracture network simulations.

Abstract

We investigate the potential impact of colloids on radionuclide transport through fractured rock at the Äspö site. Two kinetic sorption models are considered for sensitivity analysis: bi-linear and linear models. We illustrate the results for Plutonium and assume it is injected into the groundwater from a single canister at a constant rate $J_0 = 0.003$ g Pu/yr, following a random flow path to the biosphere. Without colloids, the median Pu discharge is effectively zero. For some parameter combinations, we find that colloid-facilitated transport of Pu can be significant if advective transport is relatively rapid, with Pu discharge up to 25% of the injection rate; this can be compared to 0.3% predicted by Allard et al. (1991) using a simplified (equilibrium) irreversible sorption model. For rapid advective transport, filtration with $\epsilon = 1$ 1/yr reduces Z by only a factor 20, from 25% to 1.3%. The actual *in-situ* filtration rate is currently unknown (uncertain) and would need to be determined from site-specific experiments. The linear sorption model provides a reasonable upper bound for the site-specific conditions at the Äspö site.

Chapter 1

Introduction

Colloids can be found in all types of subsurface environments, and have long been recognized as potential carriers of contaminants. Since retention of colloids is relatively low, or even non-existent, the attachment of strongly sorbing contaminants onto colloids could imply a considerably more rapid transport by groundwater than would be predicted in the absence of colloids. Most of the radionuclides of interest have a strong affinity to sorb onto crystalline rock, implying strong retention. However, colloids may facilitate more rapid transport for several radionuclides, thereby reducing the efficiency of the crystalline geosphere to act as a barrier for long-term storage of nuclear waste.

Allard et al. (1991) considered colloid-facilitated radionuclide transport (CFRT) using a simple equilibrium model for reversible as well as irreversible sorption of radionuclides on colloids. Their conclusion was that CFRT has an insignificant impact for the conditions in Swedish crystalline rock. The approach of Allard et al. (1991) may be critically viewed as over-simplistic. In particular, irreversible sorption is treated with an equilibrium model, the transport is essentially neglected and uncertainty in the results was not quantified.

Since the work of Allard et al. (1991) several studies have improved our understanding of colloid-porous media interactions as well as of colloid-solution exchanges for actinides. An important field-scale observation was the unexpectedly large Plutonium displacement from the release point at the Nevada Test Site (Kersting et al., 1999). Parallel laboratory studies have revealed rate-limited sorption on inorganic colloids for several actinides (Lu et al., 1998; Lu et al., 2000) from which kinetic rates have been inferred (Painter et al., 2002). On the theoretical side, a general stochastic modelling framework for CFRT with linear colloid-solution exchange is currently available (Cvetkovic, 2000).

Klos et al. (2002) provided the most comprehensive analysis of CFRT for Swedish conditions to date, focusing on Aberg. They assumed linear colloid-solution exchange, diffusion/sorption as the retention mechanism for dissolved radionuclides and hydrody-

namic transport governed by advection-dispersion. The colloid-solution exchange parameters were estimated using the Lu et al. (2000) laboratory data and field observations of Kersting et al. (1999), whereas the transport-retention parameters for Aberg were used from SR-97 studies. Results are summarized as breakthrough curves for various parameter ranges.

In this report we investigate the potential impact of colloid-facilitated transport of Plutonium at the Äspö site, by accounting for radionuclide retention due to diffusion/sorption. A few novel aspects of our site-specific application are as follows. First, we use data from discrete fracture simulations of Outters and Shuttle (2000) on τ and β as key hydrodynamic parameters for advection and retention (e.g., Cvetkovic et al., 2002), rather than utilize the advection-dispersion equation for field-scale hydrodynamic transport; this enables direct quantification of uncertainty due to geological heterogeneity. Second, we do not limit our analysis to the linear sorption model for colloid-solution exchange, but also consider bi-linear sorption which accounts for possible sorption limitations. Finally, in the current analysis colloids can be subject to retention and removal, i.e., we account for possible effects of combined retardation and filtration of colloids.

Potential impact of CFRT is to be quantified statistically, by computing the distribution of the total Plutonium discharge into the accessible environment (or "compliance boundary") suitably defined as the biosphere. The problem configuration is consistent with the one considered by Allard et al. (1991) where a constant injection rate of Pu due to dissolution from hypothetical failed canisters, is assumed. We introduce simple dimensionless measures of colloid impact on the barrier function of the host rock, by normalizing steady-state Pu discharge into the accessible environment with the injection rate.

Chapter 2

Modelling framework and assumptions

The basic assumptions/conditions for our present analysis are summarized as follows:

- Flow/advection:
  - Dominant hydrodynamic mode of transport is advection within fractures; small-scale dispersion is neglected.
  - Groundwater flow is at steady-state.
- Radionuclide:
  - Radionuclide is released from a canister by dissolution, at a constant rate J_0 [M/T], over a hypothesized area A_0 [L^2] with a volumetric flow rate q [L^3/T]; the boundary condition for transport is thus assumed as $J_0\, H(t)$, where $H()$ is the Heaviside step function.
  - Retention of dissolved radionuclide is only by diffusion/sorption in the rock matrix.
- Colloids:
  - Colloids can be subject to linear equilibrium retardation due to reversible attachment/detachment, and/or permanent (irreversible) removal (filtration).
  - If retardation is neglected, colloids move with groundwater velocity.
  - Irreversible removal of colloids is approximately compensated by colloidal generation, thus colloidal concentration C_c [M/L^3] along a flow path in the rock is approximately constant.

2.1 General model

The general radionuclide transport model which captures the key kinetic interactions (diffusion/sorption in the rock matrix and kinetic sorption onto colloids), is written as:

$$\frac{\partial C}{\partial t} + \nabla \cdot \mathbf{J} = \frac{\theta(\mathbf{x})\, D(\mathbf{x})}{b(\mathbf{x})} \frac{\partial C_m}{\partial z} \mid_{z=0} + \psi_c(C,S) - \lambda\, C \tag{2.1a}$$

$$\frac{\partial S}{\partial t} + \nabla \cdot (S\, \mathbf{J}_c) = \psi_s(C,S) - \lambda\, S \tag{2.1b}$$

$$R_m(\mathbf{x}) \frac{\partial C_m}{\partial t} = D(\mathbf{x}) \frac{\partial^2 C_m}{\partial z^2} - \lambda\, R_m(\mathbf{x})\, C_m \tag{2.1c}$$

The quantities given in (2.1a)-(2.1c) are:

J – mass flux vector for tracer in fracture [M/L^{2}T]

ψ_c – sink/source term for tracer in solution [M/L^{3}T]

ψ_s – sink/source term for tracer on colloids [M/L^{3}T]

b – "half-aperture" for fracture [L]

D – pore diffusivity of rock matrix [L^2/T]

θ – porosity of rock matrix [-]

C – mobile tracer concentration in fracture [M/L^3]

C_m – immobile tracer concentration in rock matrix [M/L^3]

R_m – retardation coefficient for rock matrix [-]

S – tracer concentration on colloids in fracture [M/L^3]

λ – decay rate [1/T]

z – distance perpendicular to plane of fracture [L]

x – Cartesian position vector [L]

t – time [T]

In the absence of colloids, $\psi = 0$, whereby (2.1a) and (2.1c) reduce to the well known system of equations for radionuclide transport in fractured rock (e.g., Neretnieks, 1980).

The source function ψ is in general non-linear and (2.1a)-(2.1c) need to be solved numerically. Given the fact that heterogeneity need to be accounted for, numerical solution of (2.1a)-(2.1c) may require considerable effort. In addition, it may be difficult to gain insight into the dominant effects only based on numerical simulations. For this reason, we shall simplify (2.1a)-(2.1c) in several ways. The intention is to use conservative assumptions to the extent possible, and provide relatively simple solutions which capture what we consider are most dominant effects.

2.2 Simplified retention model

Consider first the case without colloids and decay. The well-known solution of transport is given by the unit mass discharge, γ, as

$$\gamma(t) = \frac{H(t-\tau)\,\sqrt{T}}{2\sqrt{\pi}\,(t-\tau)^{3/2}}\,\exp\left[-\frac{T}{4(t-\tau)}\right] \tag{2.2}$$

where $T \equiv (\kappa\beta)^2$ is a "retention time", $\kappa \equiv \theta\sqrt{DR_m}$ is the material parameter group, and β quantifies hydrodynamic control of retention (referred to as "transport resistance"). Setting the time derivative of $\gamma(t)$ to zero, we compute the peak arrival time, t_p as

$$t_p = \tau + \frac{T}{6}$$

We may consider t_p to provide a bulk measure of radionuclide residence time, as subject to retention by unlimited diffusion/sorption. In fact, the second term on the RHS quantifies the "retardation" relative to the water residence time; it is zero if diffusion/sorption is zero, i.e., the radionuclide moves with the groundwater (τ). Introducing a bulk "retardation coefficient" R,[1] we define

$$R \equiv \frac{t_p}{\tau} = 1 + \frac{T}{6\,\tau}$$

Using the retention time T, radionuclide transport can be simplified as equilibrium retardation with R being the "retardation coefficient", i.e.,

$$\gamma_{\rm eq}(t) = \mathrm{e}^{-\lambda t}\,\delta(t-t_p) = \mathrm{e}^{-\lambda t}\,\delta(t-\tau R) \tag{2.3}$$

This assumption is not conservative in terms of the first arrival, since portions of the radionuclide will arrive earlier than t_p, however, the simplification is conservative in terms of the discharge peak, since the equilibrium approximation $\gamma_{\rm eq}$ assumes a larger peak than γ. We shall discuss this assumption/simplification more in the following sections.

2.3 Three-phase model

With the step input $J_0\,H(t)$, radionuclide discharge into the accessible environment is a monotonically increasing function of time until a steady-state is reached. Our current objective is to provide a relatively comprehensive sensitivity analysis of how different parameters affect colloid-facilitated transport quantified by the total radionuclide discharge,

[1] Note that compared to the classical equilibrium retardation model, R here is not a constant but a function of τ.

for linear and non-linear sorption models. For this purpose, we shall further simplify the transport problem by considering the steady-state limit, i.e., $t \to \infty$.

The steady-state mass balance equations for radionuclide concentration in solution (C [M/L^3]) and on colloids (S [M/L^3]) are obtained from (2.1a)-(2.1c) using equilibrium sorption with R to quantify retention due to diffusion/sorption:

$$\mathbf{V} \cdot \nabla C = \psi(C,S) - \lambda\, R(\mathbf{x})\, C \quad ; \qquad \mathbf{V} \cdot \nabla S = -\psi(C,S) - \lambda\, R_c\, S - \epsilon\, S \tag{2.4}$$

where R is the "retardation coefficient" for the radionuclide in the mobile water, due to diffusion/sorption.

In this discussion, we consider two models for the solution-colloid exchange.

1. *Linear model* for which ψ takes the form

$$\psi(C,S) = -\alpha_f\, C + \alpha_r\, S \tag{2.5}$$

   where α_f [1/T] is the forward and α_r [1/T] the reverse sorption rate; if $\alpha_r \to 0$, we recover the irreversible linear sorption model where α_f is the irreversible sorption rate.

2. *Bi-linear model* for which ψ takes the form

$$\psi(C,S) = -\alpha\, C\, (S_m - S) + \alpha_r\, S \tag{2.6}$$

   where α [L^3/MT] is a rate coefficient per unit concentration, and S_m [M/L^3] is the maximum radionuclide concentration that can sorb on colloids for a given colloidal concentration.

Using the methodology of Cvetkovic and Dagan (1994), we can transform the three-dimensional equations (2.4) to one-dimensional trajectories (streamtubes); the result is

$$\frac{d\,C}{d\,\tau} = \psi(C,S) - \lambda\, R(\tau,\beta)\, C \quad ; \qquad \frac{d\,S}{d\,\tau} = -\psi(C,S) - \lambda\, R_c\, S - \epsilon\, S \tag{2.7}$$

where τ [T] is the groundwater residence time, in this case coinciding with the colloid residence time, from the injection point to the discharge surface; the exchange rate ψ takes the forms (2.5)-(2.6).

Equations (2.7) are written in terms of radionuclide concentration. We wish to write (2.7) in terms of radionuclide *discharge*, i.e., mass per unit time as a function of τ. Multiplying the concentrations of (2.7) with the volumetric flow rate in the streamtube, q [L^3/T],

and normalizing with J_0 [M/T], we get for the linear and bi-linear sorption models:

$$\frac{d\,X}{d\,\tau} = -\psi(X,Y) - \lambda\, R(\tau,\beta)\, X \;; \quad \frac{d\,Y}{d\,\tau} = \psi(X,Y) - \lambda\, R_c\, Y - \epsilon\, Y \tag{2.8}$$

$$\psi = \alpha_f\, X - \alpha_r Y \quad \text{(linear)} \;; \quad \psi = \alpha\, X\, (Y_m - Y) - \alpha_r Y \quad \text{(bi-linear)} \tag{2.9}$$

where $Y_m \equiv S_m\, q/J_0$, $X \equiv Cq/J_0$ and $Y \equiv Sq/J_0$ are dimensionless. The parameter α in (2.9) has dimensions [1/T] and is defined as $\alpha J_0/q$; we retain the same notation for simplicity. Hence all terms in (2.8)-(2.9) have dimensions [1/T].

Equations (2.8)-(2.9) are two pairs of coupled ODEs with the following boundary conditions: $X(0) = 1$ and $Y(0) = 0$. The solutions $X(\tau)$ and $Y(\tau)$ are random variables since both β and τ are random. With X and Y computed, we obtain the total radionuclide discharge (in solution and colloid-bounded) as $Z \equiv X + Y$, which is also random due to the randomness of τ.

Chapter 3

Site-specific application

3.1 Advective transport and radionuclide

To assess the potential impact of CFRT at the Äspö site, we use a series of discrete fracture network (DFN) simulation data obtained by Outters and Shuttle (2000). DFN simulations are a well-established method for addressing flow and the resulting τ distribution in fractured rocks (Andersson and Dverstorp, 1987; Cacas et al., 1990; Nordqvist et al., 1992).

The simulations of Outters and Shuttle (2000) are specific to the Äspö HRL site, and are based on one of the most comprehensive hydraulic and structural data sets available for crystalline rocks. A hypothetical waste repository was set at approximately 500 m below the sea level, and transport of "water particles" from canisters to the discharge surface of the Baltic Sea computed. The simulations were designed to mimic as closely as possible the fracture networks in the granitic rock surrounding the Äspö HRL. We provide only a brief summary here; details can be found in Outters and Shuttle (2000).

The simulations are based on FracMan, where a large number of disk shaped fractures with pre-defined radius and orientation distribution are placed randomly throughout the simulation region in addition to deterministic fracture zones. Intersections between fractures are then identified, and fracture segments that are not on the network backbone are removed. Each of the remaining fracture segment connecting two fracture intersections is then replaced by an equivalent flow pipe or channel. Pressure boundary conditions are applied to the simulation domain and flow in the equivalent pipe network is solved numerically by assuming laminar flow in each pipe.

Once the flow network is constructed, pathways through the network are identified using the code PAWorks (Dershowitz et al., 1999) that is based on a group theory search algorithm. For the particular simulations described here, a large number of starting positions (waste canisters) are placed in a spatial pattern consistent with current repository

design. Canisters intersecting individual fractures are identified, as is the dominant pathway connecting each to the discharge plane. The possibility of downstream bifurcation in the transport pathway was neglected in these simulations. This approximation is consistent with previous network simulations and field data which suggest that fracture network flow is often highly channelized into a small number of dominant flowpaths, consistent with a flow network that is arranged in a dendritic pattern with flow converging toward larger and larger conductive features. Moreover, the no-branching hypothesis tends to overestimate the peak concentrations (by underestimating dilution effects) and is thus an important bounding approximation that is used in applications. Once each particle trajectory is identified, the length, aperture, and velocity for each segment is recorded.

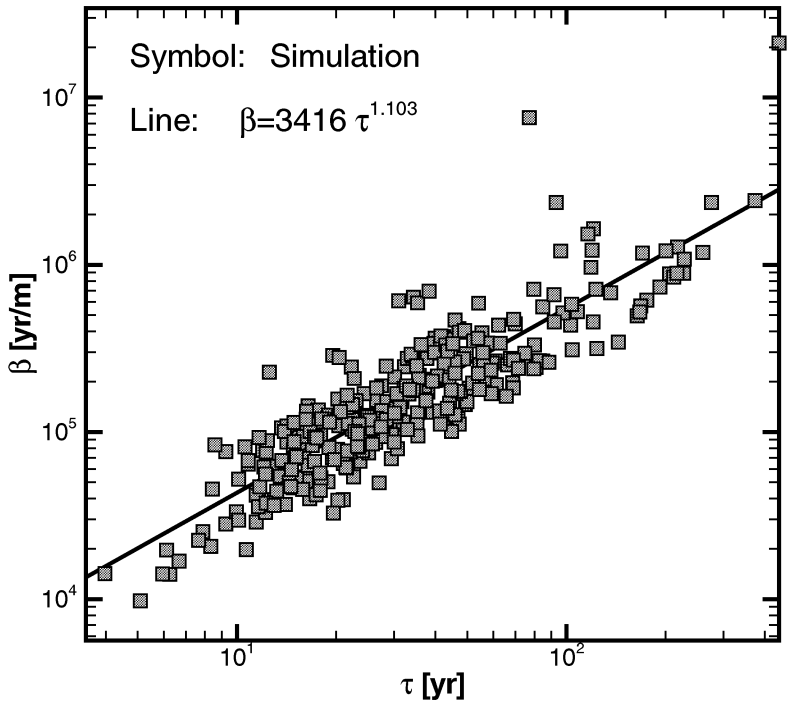

Figure 3.1: Scatter plot for τ, β obtained from DFN simulation results of Outters and Shuttle (2000).

A statistical data base of τ and β was obtained from the DFN simulations. Relatively strong correlation between τ and β was found, as indicated by the scatter plot in Figure 3.1. The best fit on the log-log plot is a line with $\beta = 3416\,\tau^{1.103}$, which we approximate here as $\beta = k\tau$ with $k = 3400$ 1/m. The simulated τ distribution and correlation can then be used directly to compute the distribution of the total radionuclide discharge $Z \equiv X + Y$,

where X and Y are computed from (2.8) -(2.9).

For illustration purposes, we consider Pu-239 and use the sorption coefficient of 1 m^3 kg^{-1} (Andersson, 1999) as a representative value. The pore diffusivity is assumed as $D = 5.2 \cdot 10^{-9}$ m^2/yr and the matrix porosity as $\theta = 0.004$. The half-life of Pu is 2.4×10^4 yr which yields $\lambda = 3 \cdot 10^{-5}$ 1/yr.

3.2 Sorption of radionuclide on colloids

Colloidal concentration C_c is available from borehole measurements at various locations at the Äspö site; C_c was found to depend strongly on salinity. From Figure 5 in Laaksoharju (2002, "Status report of the colloid experiment at Äspö HRL tunnel in Sweden", unpublished), we select $C_c = 0.025$ mg/L from borehole KA3110A for moderate salinity of 3000 mg Cl^-/L as representative for the Äspö site. For these conditions, we would need to determine the maximum Pu mass that can sorb on the 0.025 mg of colloids in one liter of groundwater, here denoted by S_m.

For the alluvial aquifer south of Yucca Mnt., Nevada, we established $C_c = 0.6$ mg/L as the representative value, i.e., factor 20 greater colloidal concentration than at the Äspö site. S_m was estimated for the alluvial aquifer in two different ways, which yielded a wide range for S_m as 10^{-7}-10^{-4} g Pu/L (Cvetkovic et al., in prep.). To obtain the upper limit of $S_m = 10^{-4}$ g Pu/L, the measured size distribution of colloids was used jointly with the assumption of spherical particles; the result was a surface area per unit ground water volume. Davis and Kent (1990) recommend a value of 2.3 sites/nm^2 (sites per unit area), which was used to compute S_m assuming that sorption of Plutonium on colloids is monolayer, mononuclear (1 atom Pu per sorbed complex) and monodentate (1 complex sorbed per site). The lower limit of $S_m = 10^{-7}$ g Pu/L was obtained using calculated K_d for Pu on colloids in the alluvial aquifer based on water chemistry, colloid concentration, colloid size distribution and sorption modelling (Contardi et al., 2001).

The assumed "representative" colloidal concentration for the Äspö site of $C_c = 0.025$ mg/L is approximately an order of magnitude lower than the corresponding value for the alluvial aquifer at Yucca Mnt. ($C_c = 0.6$ mg/L). Rather than attempt to estimate S_m for $C_c = 0.025$ mg/L, we shall assume that for the Äspö site S_m is in the range 10^{-8}-10^{-5} g Pu/L, which is 10 times lower than what was determined for the alluvial aquifer, Yucca Mnt., consistent with the fact that the colloidal concentration is an order of magnitude lower at Äspö. Thus we assume roughly a linear dependence of S_m on C_c, which is rea-

sonable given the low concentrations in question. In our following calculations, we shall consider the two limiting values of S_m as 10^{-8} g Pu/L and 10^{-5} g Pu/L.

Based on experimental data of Lu et al. (1998, 2000), an "irreversible" sorption rate α_f for Pu on inorganic colloids (hematite, monmorillonite, smectite and silicate) was estimated in the range $\alpha_f = 0.002-0.018$ 1/h (Painter et al., 2002). The experimental data was available for a limited range of relatively high colloidal concentrations, and our data evaluation could not establish a dependence of the sorption rate α_f on the colloidal concentration C_c. However, based on a linear relationship between α_f and C_c (Saiers and Hornberger, 1996), we estimated $\alpha_f = 0.1$ 1/yr as a representative (fixed) value for the alluvial aquifer (Cvetkovic et al., in prep). Here, we shall consider the range $\alpha_f = 0.001 - 0.1$ 1/yr for sensitivity analysis. In Cvetkovic et al. (in prep) it was shown that the irreversible model always yields a larger effect of CFRT compared to a corresponding reversible model (i.e., with the same forward sorption rate α_f but finite reverse rate). Thus we shall simplify the present analysis by considering the irreversible (conservative) limit, i.e., $\alpha_r \to 0$, whereby α_f becomes the irreversible sorption rate.

3.3 Colloid retardation and filtration

Site-specific data on R_c and ϵ for natural colloids at the Äspö site is currently unavailable. A distribution of possible R_c values was estimated for the alluvial aquifer at Yucca Mnt. using filtration theory and an assumed detachment rate, with the median of approximately $R_c = 20$ (Wolfsberg and Reimus, 2000). In our following calculations, we shall neglect the effect of colloidal (equilibrium) retardation and assume $R_c = 1$. We note that the impact of R_c on CFRT for Pu was found to be modest in the alluvial aquifer (Cvetkovic et al., in prep).

The irreversible removal (filtration) rate ϵ has a potentially significant effect on CFRT and is here treated as a sensitivity parameter in the range ϵ =0–1 1/yr.

3.4 Injection conditions

Our basic concept for transport is a flow path (streamtube) extending from a single canister through the fractured rock to the accessible environment. The two basic parameters to be hypothesized here are the Plutonium injection rate J_0 and the volumetric flow rate q for a single flow path; both parameters depend on the scenario of Pu release.

Our objective here is to highlight the role of the fractured rock as a barrier to Plutonium

with regard to colloid-facilitated transport, rather than detailed modelling of a hypothetical radionuclide release which can be found elsewhere. We therefore assume a cross-sectional area A_0 for the hypothetical failed canister over which the injection into the transport (flow) path takes place, and the Pu mass injection rate, with a ratio of $J_0/A_0 = 3$ g Pu/(yr m^2). For a release area of say $A_0 = 0.001$ m^2, for instance, the assumed ratio yields $J_0 = 0.003$ g Pu/yr; this injection rate is consistent with that assumed by Allard et al. (1991).

The volumetric flow rate q for a single flow path is assumed perfectly correlated to the groundwater residence time and computed as $q = A_0\,\ell/\tau$, where $\ell = 500$ m is approximately the transport distance. A more rigorous approach would be to relate q to the Eulerian velocity at the injection point, and then use a joint probability density function for this velocity and the groundwater residence time. Such an approach would require additional parameters and/or assumptions, and we therefore do not consider it warranted for our current purpose.

3.5 Transport model

The bi-linear model is given in (2.9), however, in this case the normalized maximum discharge Y_m is a function of τ, since q is assumed to be a function of τ. Furthermore, $\alpha_f = Y_m\alpha$ is assumed fixed (i.e., independent of τ). The site-specific transport equations for the bi-linear model (2.9) are then formulated in the irreversible limit as:

$$\frac{d\,X}{d\,\tau} = -\alpha_f\,X + X\,Y\,\left(\frac{\alpha_f\,J_0\,\tau}{\ell\,A_0\,S_m}\right) - \lambda\,R(\tau)\,X$$

$$\frac{d\,Y}{d\,\tau} = \alpha_f\,X - X\,Y\,\left(\frac{\alpha_f\,J_0\,\tau}{\ell\,A_0\,S_m}\right) - \lambda\,R_c\,Y - \epsilon\,Y \tag{3.1}$$

where values for all parameters have been specified in the preceding subsections and $R(\tau) = 1 + T/6\tau = 1 + (\kappa k)^2\,\tau/6$. Equations (3.1) are solved using the Runge-Kutta method, and the normalized total Pu discharge is computed as $Z = X + Y$.

Linearization of sorption in (3.1) yields

$$\frac{d\,X}{d\,\tau} = -\alpha_f\,X - \lambda\,R(\tau)\,X$$

$$\frac{d\,Y}{d\,\tau} = \alpha_f\,X - \lambda\,Y - \epsilon\,Y \tag{3.2}$$

in view of $R_c = 1$. A transient version of (3.2) (with R constant) has been presented in Cvetkovic (2000) .

With $X(0) = 1$ and $Y(0) = 0$, and $R(\tau) = 1 + (\kappa k)^2 \tau/6$, we can solve (3.2) to get

$$X(\tau) = \mathrm{e}^{-\alpha_f \tau - B\tau^2}$$

$$Y(\tau) = \mathrm{e}^{-A\tau + (\alpha_f - A)^2/4B}\, \alpha_f \frac{\sqrt{\pi}}{2\sqrt{B}} \left\{ \Phi\left[\sqrt{B} \left(\tau + \frac{\alpha_f - A}{2B} \right) \right] - \Phi\left(\frac{\alpha_f - A}{2\sqrt{B}} \right) \right\} \tag{3.3}$$

where

$$A \equiv \epsilon + \lambda \qquad B \equiv \frac{\lambda(\kappa k)^2}{12}$$

and Φ is the error function defined by

$$\Phi(x) \equiv \frac{2}{\sqrt{\pi}} \int_0^x \mathrm{e}^{-y^2}\, dy = \frac{2}{\sqrt{\pi}}\, \mathrm{e}^{-x^2} \sum_{i=0}^{\infty} \frac{2^i\, x^{2i+1}}{(2i+1)!!}$$

Chapter 4

Discussion of results

4.1 Approximation of retention

We first wish to assess the accuracy of the linearization $\beta = 3400\tau$ using the simulated τ in Outters and Shuttle (2000). In Figure 4.1 we compare the CCDFs and CDFs for β as obtained directly from simulations (curve denoted as "simulations" in Figure 4.1) with approximation $\beta = k\tau$, $k = 3400$ 1/m using simulated τ (curve denoted as "approximate" in Figure 4.1).

We find that the low β values (tail of CDF) are relatively well approximated by the linearized expression if the simulated τ is used. The large values of β (tail of CCDF) are underestimated by the linearization, in particular for CCDF less than 10%. This is due to the fact that high β values show greater statistical persistence (power-law tail) in comparison to water residence time τ.

To assess the implications of the linearization $\beta = k\tau$ on tracer transport with diffusion/sorption, we compare exact and approximate expected cumulative discharge. Specifically, the exact value is obtained from $\langle \int_0^t \gamma dt' \rangle$ where γ is given in (2.2) (curve denoted as "exact" in Figure 4.2). The approximate expected cumulative discharge is obtained from $\langle \int_0^t \gamma_{\rm eq} dt' \rangle$ where $\gamma_{\rm eq}$ is given in (2.3). We consider two approximate cases, one where both τ and β are used from simulations (curve denoted by "approx ($\tau\&\beta$)" in Figure 4.2), and the other where we employ $\beta = 3400\tau$ (Figure 3.1), and use τ from simulations (curve denoted as "approx ($\tau\&k\tau$)" in Figure 4.2).

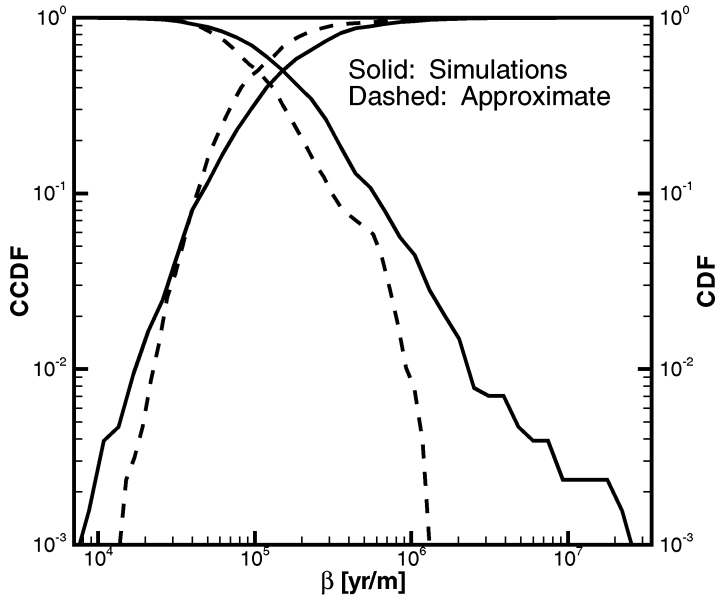

Figure 4.1: Comparison of the simplified retention model with the "exact" transport model, (a) CCDF for β, (b) expected cumulative breakthrough.

The approximate expression (2.3) with τ, β from simulations has essentially an identical form as the "exact" curve, however, it is shifted toward the left (Figure 4.2); thus the cumulative breakthrough is predicted somewhat earlier. The approximate cumulative breakthrough where $\beta = 3400\tau$ deviates more from the "exact" curve, exhibiting less spreading; hence early arrival is overestimated and late arrival underestimated. Nevertheless, both approximations provide reasonable estimates for the purpose of assessing the potential impact of colloid-facilitated Pu transport.

4.2 Deterministic results with linear model

In the previous section, we compared the exact and and approximate expected cumulative discharge without considering the colloids, and found that the approximations provide a reasonable alternative to the exact case (Figure 4.2). In this section, we take advantage of this fact and use (3.1) or (3.2) assuming equilibrium retardation as given in (2.3), to assess the potential impact of colloids by computing the total radionuclide discharge $Z = X + Y$.

In Figure 4.3 we illustrate the dependence of the normalized total Pu discharge on water residence time τ, in the interval 1-440 years (which is approximately the interval in which simulated τ fall) for different combinations of filtration rate ϵ and irreversible

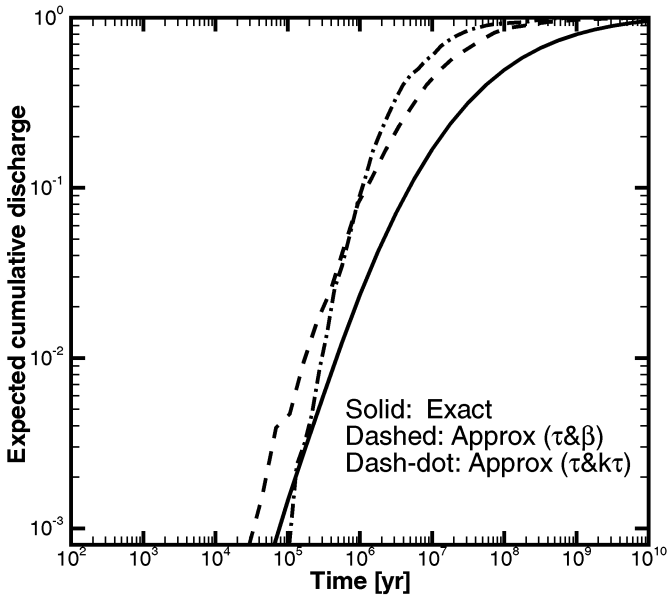

Figure 4.2: Comparison of the simplified retention model with the "exact" transport model, (a) CCDF for β, (b) expected cumulative breakthrough.

sorption rate α_f, using the linear irreversible sorption model. This model was shown to be most conservative, compared to the bi-linear and/or reversible sorption models (Cvetkovic et al., in prep.; see also next section).

Six combinations of ϵ, α_f are considered, in the interval 0.001-0.1 1/yr. In Figure 4.3 we also plot the (constant) value predicted by Allard et al. (1991) of $Z = 0.003$. In addition, we plot the complementary cumulative distribution function (CCDF) of τ in order to expose the likeliness of τ values (RHS axis in Figure 4.3), according to the DFN simulations of Outters and Shuttle (2000).

For lowest α_f and ϵ, the predicted Z agrees surprisingly well with the value of Allard et al. (1991), over the entire range of water residence times (10-440 years) (Figure 4.3a). For low α_f and large ϵ, the predicted Z is significantly lower than 0.003 almost over the entire τ range (Figure 4.3b). For a low ϵ and moderate α_f, the predicted Z is above 0.003 almost one order of magnitude in the whole τ interval (Figure 4.3c). Increase in ϵ reduces significantly the effect of colloids on Pu discharge, such that it is above 0.003 approximately in the interval $1 < \tau < 33$ years, and below 0.003 for $\tau > 33$ years (Figure 4.3d). Relatively small filtration rate ϵ, with a large irreversible rate α_f, results in large Z almost two orders of magnitude larger than predicted by Allard et al. (1991) (Figure 4.3e). Large ϵ and α_f result in $Z > 0.003$ for $\tau < \tau_{\text{median}}$ and $Z < 0.003$ for

$\tau > \tau_{\text{median}}$ (Figure 4.3e); we estimate τ_{median} as 40 years.

4.3 Statistical results

In the previous section we computed $Z = Z(\tau)$ as a deterministic function. Given the probability density function of τ, $f(\tau)$, we compute the probability density function of Z using the well-known relationship $f(Z) = |d\tau/dZ|\, f[\tau(Z)]$. Using this relationship as $f(z)dz = f(\tau)d\tau$ in conjunction with the fact that Z is a mononononically decreasing function of τ (Figure 4.3), we evaluate the CCDF of the total normalized Pu discharge, Z, as

$$\text{CCDF}(Z) = 1 - \text{CCDF}(\tau)$$

where $Z(\tau)$ is obtained either from (3.1) or from (3.3). We compute CCDF(Z) for the range of rates ϵ and α_f corresponding to those for the linear model in Figure 4.3, where in addition we include the dependence on the maximum sorbed concentration S_m for the two limiting values, 10^{-8} g Pu/L and 10^{-5} g Pu/L. The 1 percentile of Z is defined as Z for which CCDF is 0.99, the median as Z for which the CCDF is 0.5 and 99% percentile as Z for which the CCDF is 0.01. For comparison we note that the value predicted by Allard et al. (1991) is 0.003.

Table 4.1: The 1 percentile for total normalized Pu discharge Z for different S_m and irreversible removal rate ϵ, using the bi-linear and linear sorption models.

ϵ [1/yr]	α_f [1/yr]	$S_m = 10^{-8}$ [g Pu/L]	$S_m = 10^{-5}$ [g Pu/L]	Linear Model
0	0.001	.4875E-03	.2750E-02	.2808E-02
	0.01	.2675E-03	.2656E-01	.2763E-01
	0.1	–	.2000E+00	.2369E+00
0.001	0.001	.3674E-03	.2069E-02	.2113E-02
	0.01	.2022E-03	.1999E-01	.2079E-01
	0.1	.1519E-03	.1505E+00	.1783E+00
0.01	.001	.2882E-04	.1603E-03	.1637E-03
	.01	.1629E-04	.1548E-02	.1611E-02
	0.1	–	.1166E-01	.1379E-01
0.1	0.001	.2574E-15	.1258E-14	.1287E-14
	0.01	.1881E-15	.1215E-13	.1264E-13
	0.1	.1735E-15	.9094E-13	.1066E-12
1	0.001	.1261E-43	.1261E-43	.0000E+00
	0.01	.1261E-43	.1261E-43	.0000E+00
	0.1	.1261E-43	.1261E-43	.0000E+00

Table 4.2: The median for total normalized Pu discharge Z for different S_m and irreversible removal rate ϵ, using the bi-linear and linear sorption models.

ϵ [1/yr]	α_f [1/yr]	$S_m = 10^{-8}$ [g Pu/L]	$S_m = 10^{-5}$ [g Pu/L]	Linear Model
0	0.001	.4911E-03	.2770E-02	.2828E-02
	0.01	.2695E-03	.2676E-01	.2783E-01
	0.1	–	.2015E+00	.2387E+00
0.001	0.001	.4781E-03	.2693E-02	.2750E-02
	0.01	.2631E-03	.2601E-01	.2706E-01
	0.1	.1976E-03	.1959E+00	.2320E+00
0.01	0.001	.3756E-03	.2089E-02	.2133E-02
	0.01	.2122E-03	.2018E-01	.2099E-01
	0.1	–	.1519E+00	.1797E+00
0.1	0.001	.3400E-04	.1662E-03	.1701E-03
	0.01	.2485E-04	.1605E-02	.1671E-02
	0.1	.2292E-04	.1201E-01	.1409E-01
1	0.001	.4316E-14	.6305E-14	.6660E-14
	0.01	.1991E-13	.5993E-13	.6357E-13
	0.1	.6231E-13	.3790E-12	.4078E-12

An increase of the irreversible sorption rate α_f in the range 0.001-0.1 1/yr has effectively no impact on Z for small S_m. An increase of the irreversible sorption rate α_f in the range 0.001-0.1 1/yr however can increase Z significantly for large S_m, almost two orders of magnitude for the 1 percentile (Table 4.1) and the median (Table 4.2), and one order of magnitude for the 99 percentile (Table 4.3). An increase of the filtration rate ϵ in the range 0-1 1/yr reduces the impact of colloids, effectively eliminating it for $\epsilon \geq 1$ 1/yr when considering the 1 percentile and median of Z. The 99 percentile of Z however is still significant even for $\epsilon = 1$ 1/yr, i.e., increase in ϵ in the range 1-0 1/yr has little impact on the 99 percentile of Z (Table 4.3). This is because the 99 percentile corresponds to early arrival times (low τ) of a few years, which are not sufficient to allow filtration to be effective even with the maximum considered value of $\epsilon = 1$ 1/yr. As a rule, decrease of the maximum concentration S_m reduces the effect of CFRT. However, the impact of S_m for the considered parameter ranges is modest for the 1 percentile and median Z (one order of magnitude difference, Tables 4.1-4.2), and is insignificant for the 99 percentile (Table 4.3). From Tables 4.1-4.3, we see that the linear sorption model provides a good approximation of the transport as predicted with the bi-linear sorption model; for large S_m the two models provide essentially indistinguishable predictions over the entire CCDF range.

Table 4.3: The 99 percentile for total normalized Pu discharge Z for different S_m and irreversible removal rate ϵ, using the bi-linear and linear sorption models.

ϵ [1/yr]	α_f [1/yr]	$S_m = 10^{-8}$ [g Pu/L]	$S_m = 10^{-5}$ [g Pu/L]	Linear Model
0	0.001	.1467E-01	.1681E-01	.1787E-01
	0.01	.1447E-01	.3998E-01	.4191E-01
	0.1	–	.2110E+00	.2461E+00
0.001	0.001	.1467E-01	.1680E-01	.1785E-01
	0.01	.1447E-01	.3985E-01	.4178E-01
	0.1	.2322E-01	.2100E+00	.2450E+00
0.01	0.001	.1465E-01	.1668E-01	.1773E-01
	0.01	.1447E-01	.3873E-01	.4061E-01
	0.1	–	.2014E+00	.2347E+00
0.1	0.001	.1451E-01	.1578E-01	.1682E-01
	0.01	.1442E-01	.2996E-01	.3140E-01
	0.1	.1899E-01	.1341E+00	.1544E+00
1	0.001	.1413E-01	.1412E-01	.1512E-01
	0.01	.1411E-01	.1394E-01	.1492E-01
	0.1	.1165E-01	.1227E-01	.1292E-01

In Tables 4.4- 4.6, we normalize our computed Z from Tables 4.1-4.3 with 0.003 of Allard et al. (1991) to directly compare the two predictions. For relatively large water residence times (1 percentile and median of Z), the prediction of Allard et al. (1991) is one to two orders of magnitude larger than our predictions (i.e., conservative) for low S_m, irrespective of the filtration rate α_f (Tables 4.1 and 4.2). For large S_m and moderate to low ϵ, however, $Z > 0.003$, in particular for moderate to large sorption rate α_f (Tables 4.4 and 4.5). In fact for $\alpha_f \geq 0.01$ 1/yr and $\epsilon \leq 0.01$ 1/yr, Z obtained with the kinetic sorption model is greater than 0.003 up to two orders of magnitude (Tables 4.4-4.5). For relatively rapid water residence times (99 percentile of Z), Z obtained with the kinetic sorption model is greater than 0.003 for the entire parameter range considered, in particular for large S_m and α_f, and weak filtration (small ϵ) (Table 4.6).

Table 4.4: The 1 percentile for total normalized Pu discharge Z for different S_m and irreversible removal rate ϵ, normalized with the value 0.003 of Allard et al., using the bi-linear and linear sorption models.

ϵ [1/yr]	α_f [1/yr]	$S_m = 10^{-8}$ [g Pu/L]	$S_m = 10^{-5}$ [g Pu/L]	Linear Model
0	0.001	0.16	0.92	0.94
	0.01	0.09	8.85	9.21
	0.1	–	66.68	78.97
0.001	0.001	0.12	0.69	0.7
	0.01	0.07	6.66	6.93
	0.1	0.05	50.18	59.42
0.01	0.001	0.01	0.05	0.05
	0.01	0.01	0.52	0.54
	0.1	–	3.89	4.60
0.1	0.001	0	0	0
	0.01	0	0	0
	0.1	0	0	0
1	0.001	0	0	0
	0.01	0	0	0
	0.1	0	0	0

Table 4.5: The median for total normalized Pu discharge Z for different S_m and irreversible removal rate ϵ, normalized with the value 0.003 of Allard et al., using the bi-linear and linear sorption models.

ϵ [1/yr]	α_f [1/yr]	$S_m = 10^{-8}$ [g Pu/L]	$S_m = 10^{-5}$ [g Pu/L]	Linear Model
0	0.001	0.16	0.92	0.94
	0.01	0.09	8.92	9.28
	0.1	–	67.18	79.56
0.001	0.001	0.16	0.90	0.92
	0.01	0.09	8.67	9.02
	0.1	0.07	65.30	77.33
0.01	0.001	0.13	0.70	0.71
	0.01	0.07	6.73	7.00
	0.1	–	50.63	59.90
0.1	0.001	0.01	0.06	0.06
	0.01	0.01	0.53	0.56
	0.1	0.01	4.00	4.70
1	0.001	0	0	0
	0.01	0	0	0
	0.1	0	0	0

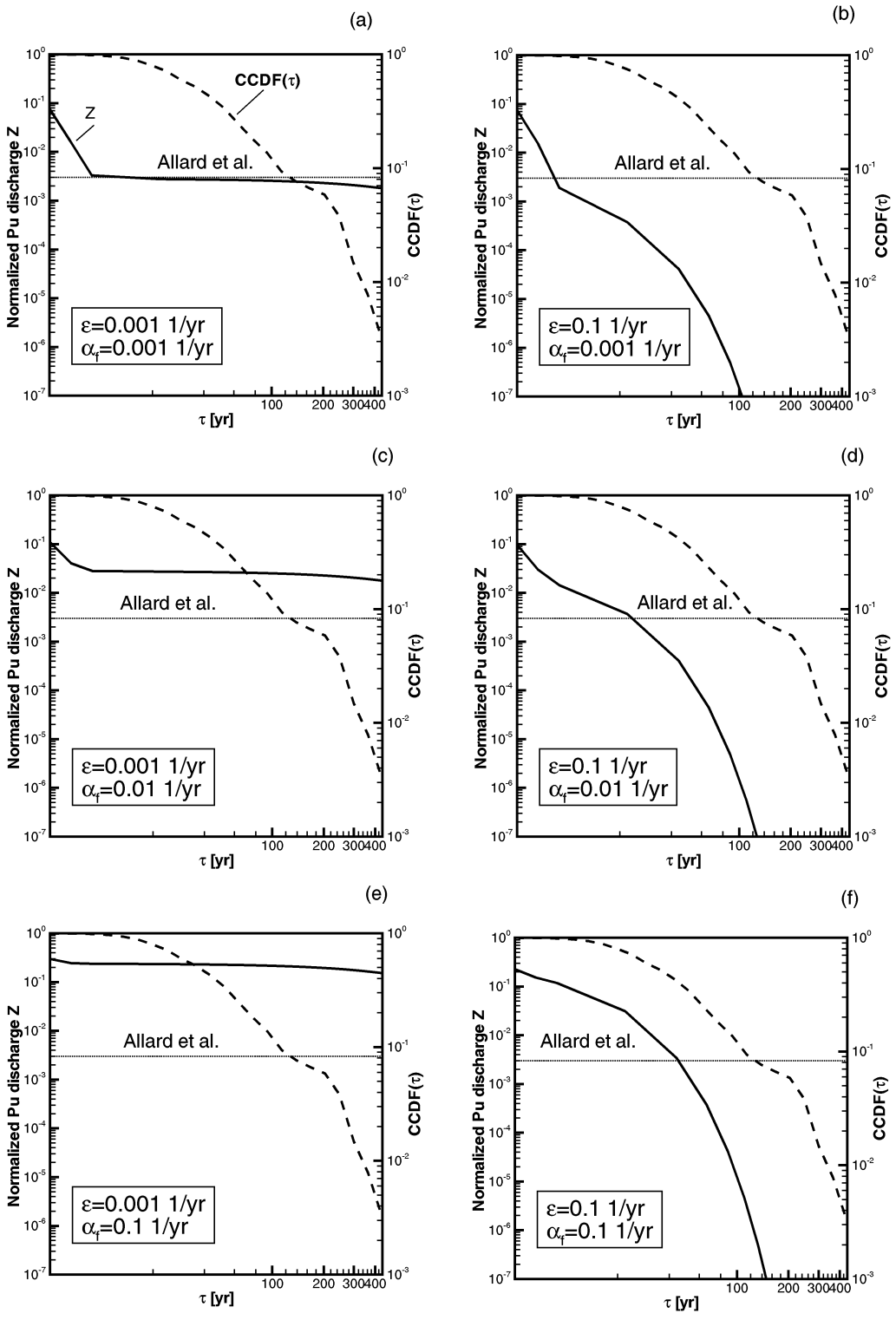

Figure 4.3: Comparison of Z as a function of τ with the prediction of Allard et al. result ($Z = 0.003$) for different α_f and ϵ, using the linear sorption model.

Table 4.6: The 99 percentile for total normalized Pu discharge Z for different S_m and irreversible removal rate ϵ, normalized with the value 0.003 of Allard et al., using the bi-linear and linear sorption models.

ϵ $[1/\mathrm{yr}]$	α_f [1/yr]	$S_m = 10^{-8}$ [g Pu/L]	$S_m = 10^{-5}$ [g Pu/L]	Linear Model
0	0.001	4.89	5.60	5.96
	0.01	4.82	13.33	13.97
	0.1	–	70.32	82.05
0.001	0.001	4.89	5.60	5.95
	0.01	4.82	13.28	13.93
	0.1	7.74	69.99	81.66
0.01	0.001	4.88	5.56	5.91
	0.01	4.82	12.91	13.54
	0.1	–	67.13	78.23
0.1	0.001	4.84	5.26	5.61
	0.01	4.81	9.99	10.47
	0.1	6.33	44.69	51.48
1	0.001	4.71	4.71	5.04
	0.01	4.70	4.65	4.97
	0.1	3.88	4.09	4.31

Chapter 5

Summary and conclusions

We investigated the potential impact of colloids on transport of Pu from a hypothetical failed canister to the accessible environment, at the Äspö site. Our general configuration is consistent with that of Allard et al. (1991) and our objective was to compare their predictions based on an equilibrium sorption model, with predictions based on a kinetic sorption model.

The total normalized Pu discharge as predicted by Allard et al. (1991) is 0.003, and was based on essentially one parameter: sorption coefficient for Pu. In our analysis, the three controlling parameters are α_f (irreversible sorption rate), ϵ (filtration rate) and S_m (maximum sorbed concentration of Pu on available colloids, here assumed to be 0.025 mg/L for the Äspö site). We computed the total normalized Pu discharge Z for a relatively wide range of α_f, ϵ and S_m values. Both deterministic and statistical results were presented.

If filtration rate ϵ is low, and maximum Pu concentration S_m and sorption rate α_f are relatively large, we found that colloid-facilitated transport of Pu is significant, with Pu discharge up to 25% of the injection rate, provided that advective transport is relatively rapid (short water residence times); 25% is almost two orders of magnitude larger than 0.3% predicted by Allard et al. (1991). Furthermore, for short water residence times, large changes in all the three parameters S_m, α_f and ϵ have a comparatively modest impact on CFRT, indicating that for such conditions, our modelling approach is insensitive to these parameters. Filtration rate ϵ is the most sensitive parameter; $\epsilon \geq 1$ 1/yr effectively eliminates the impact of colloids, for moderate to large water residence times. For rapid transport (i.e., small τ, Table 4.3), filtration with $\epsilon = 1$ 1/yr reduces Z by a factor 20, from 25% to 1.3%.

In this study, we addressed the sensitivity of the expected cumulative discharge Z on the system parameters S_m, α_f and ϵ, as summarized in the Tables and in Figure 4.3. In the least favourable case of low ϵ and high α_f (Figure 4.3e), a value of around $Z = 0.2$ is sure,

implying that the barrier function of the geosphere is significantly reduced in comparsion to the case without colloids, for which $Z = X$ is more than 20 orders of magnitude smaller. The most favourable case considered is high ϵ and low α_f (Figure 4.3b), with the probability of around 3% that $Z > 0.003$ (which is the limit estimated by Allard et al., 1991). The uncertainty in Z follows from the uncertainty in water residence times, which in turn follows the from spatial variability in the hydraulic rock properties. There are other uncertainties, however, notably in the parameters S_m, α_f and ϵ, which may significantly increase the uncertainty in Z. The knowledge of statistical distributions of S_m, α_f and ϵ would be required in order to compute the full statistics of Z.

For a more comprehensive analysis of the potential impact of CFRT in crystalline rocks, several issues need to be addressed. For instance, we neglected reversibility, which is a conservative assumption. If the impact of CFRT as predicted by our analysis is considered too large from a PA/SA perspective, then more realistic calculations (steady-state and/or transient) could be carried out assuming a (linear or bi-linear) reversible sorption model; reversibility has been shown to reduce the significance of CFRT (Cvetkovic et al., in prep.) Similarly, sorption parameters S_m and α_f need to be estimated from field and laboratory experiments, as well as based on theoretical consideration.

In this study, we considered the filtration rate to be a sensitivity parameter in the range 0-1 1/yr. Given its significance, the filtration rate ϵ would need to be estimated for field conditions. The currently planned field experiments on transport of colloids in fractures on 5-10 m scale can provide a unique opportunity for quantifying colloid retention in crystalline fractures, and in particular for inferring the filtration rate ϵ.

Bibliography

Andersson, J. (1999). SR-97: Data and data uncertainties. TR 99-09, Swedish Nuclear Fuel and Waste Management Co.(SKB).

Andersson, J. and Dverstorp, B. (1987). Conditional simulation of fluid flow in three-dimensional networks of discrete fractures. *Water Resources Research*, 23(10):1876–1886.

Cacas, M. C., Ledoux, E., de Marsily, G., Barbreau, A., Calmels, P., Gaillard, B., and Margritta, R. (1990). Modeling fracture flow with a stochastic discrete fracture network: Calibration and validation, 2. the transport model. *Water Resources Research*, 20(3):491–500.

Contardi, J., Turner, D., and Ahn, T. (2001). Modeling colloid transport for performance assessment. *Journal of Contaminant Hydrology*, 47:323–333.

Cvetkovic, V. (2000). Colloid-facilitated tracer transport by steady random ground-water flow. *Phys. Fluids*, 12:2279–2294.

Cvetkovic, V. and Dagan, G. (1994). Transport of kinetically sorbing solute by steady random velocity in heterogeneous porous formations. *Journal of Fluid Mechanics*, 265:189–215.

Cvetkovic, V., Painter, S., and Selroos, J. (2002). Comparative measures for radionuclide containment in the crystalline geosphere. *Nuclear Science and Engineering*, 142:292–304.

Davis, J. and Kent, D. (1990). *Surface complexation modeling in aqueous geochemistry*. Mineralogical Society of America, Washington, D.C.

Dershowitz, B., Eiben, T., Follin, S., and Andersson, J. (1999). SR 97 - alternative models project. Discrete fracture network modelling for performance assessment of Aberg. R 99-43, Swedish Nuclear Fuel and Waste Management Co.(SKB).

Kersting, A., Efured, D., Finnegan, D., Rokop, D., Smith, D., and Thompson, J. (1999). Migration of plutonium in ground water at the Nevada Test Site. *Nature*, 397:56–59.

Klos, R., White, M., Wickham, S., Bennett, D., and Hicks, T. (2002). Quantitative assessment of the potential significance of colloids to the KBS-3 disposal concept. Technical Report SKI 02:34, Swedish Nuclear Inspectorate (SKI).

Lu, N., Conca, J., Parker, G., Leonard, P., Moore, B., Strietelmeier, B., and Triay, I. (2000). Adsorption of actinides onto colloids as a function of time, temmperature, ionic strength, and colloid concentration. Technical Report LA-UR-00-5121, Los Alamos National Laboratory.

Lu, N., Triay, I., Cotter, C., H.D.Kitten, and Bentley, J. (1998). Reversibility of sorption of Plutonium-239 onto colloids of Hematite, Goethite, Smectite and Silica: A milestone final report of YMP. Technical Report LA-UR-98-3057, Los Alamos National Laboratory.

Neretnieks, I. (1980). Diffusion in the rock matrix: An important factor in radionuclide retention. *Journal of Geophysical Research*, 85(B8):4379–4397.

Nordqvist, A. W., Tsang, Y. M., Tsang, C. F., Dverstorp, B., and Andersson, J. (1992). A variable aperture fracture network model for flow and transport in fractured rock. *Water Resources Research*, 28(6):1703–1713.

Outters, N. and Shuttle, D. (2000). Sensitivity analysis of a discrete fracture network model for performance assessment of aberg. R 00-48, Swedish Nuclear Fuel and Waste Management Co.(SKB).

Painter, S., Cvetkovic, V., Turner, D., and Pickett, D. (2002). Significance of kinetics for sorption on inorganic colloids: Modeling and experimental considerations. *Environmental Science and Technology*. in press.

Saiers, J. and Hornberger, G. M. (1996). The role of colloidal kaolinite in the transport of cesium through laboratory sand columns. *Water Resources Research*, 32:33–41.